Cell Reports, Volume *37*

Supplemental information

Paired heavy- and light-chain signatures contribute to potent SARS-CoV-2 neutralization in public antibody responses

Bailey B. Banach, Gabriele Cerutti, Ahmed S. Fahad, Chen-Hsiang Shen, Matheus Oliveira De Souza, Phinikoula S. Katsamba, Yaroslav Tsybovsky, Pengfei Wang, Manoj S. Nair, Yaoxing Huang, Irene M. Francino-Urdániz, Paul J. Steiner, Matías Gutiérrez-González, Lihong Liu, Sheila N. López Acevedo, Alexandra F. Nazzari, Jacy R. Wolfe, Yang Luo, Adam S. Olia, I-Ting Teng, Jian Yu, Tongqing Zhou, Eswar R. Reddem, Jude Bimela, Xiaoli Pan, Bharat Madan, Amy D. Laflin, Rajani Nimrania, Kwok-Yung Yuen, Timothy A. Whitehead, David D. Ho, Peter D. Kwong, Lawrence Shapiro, and Brandon J. DeKosky

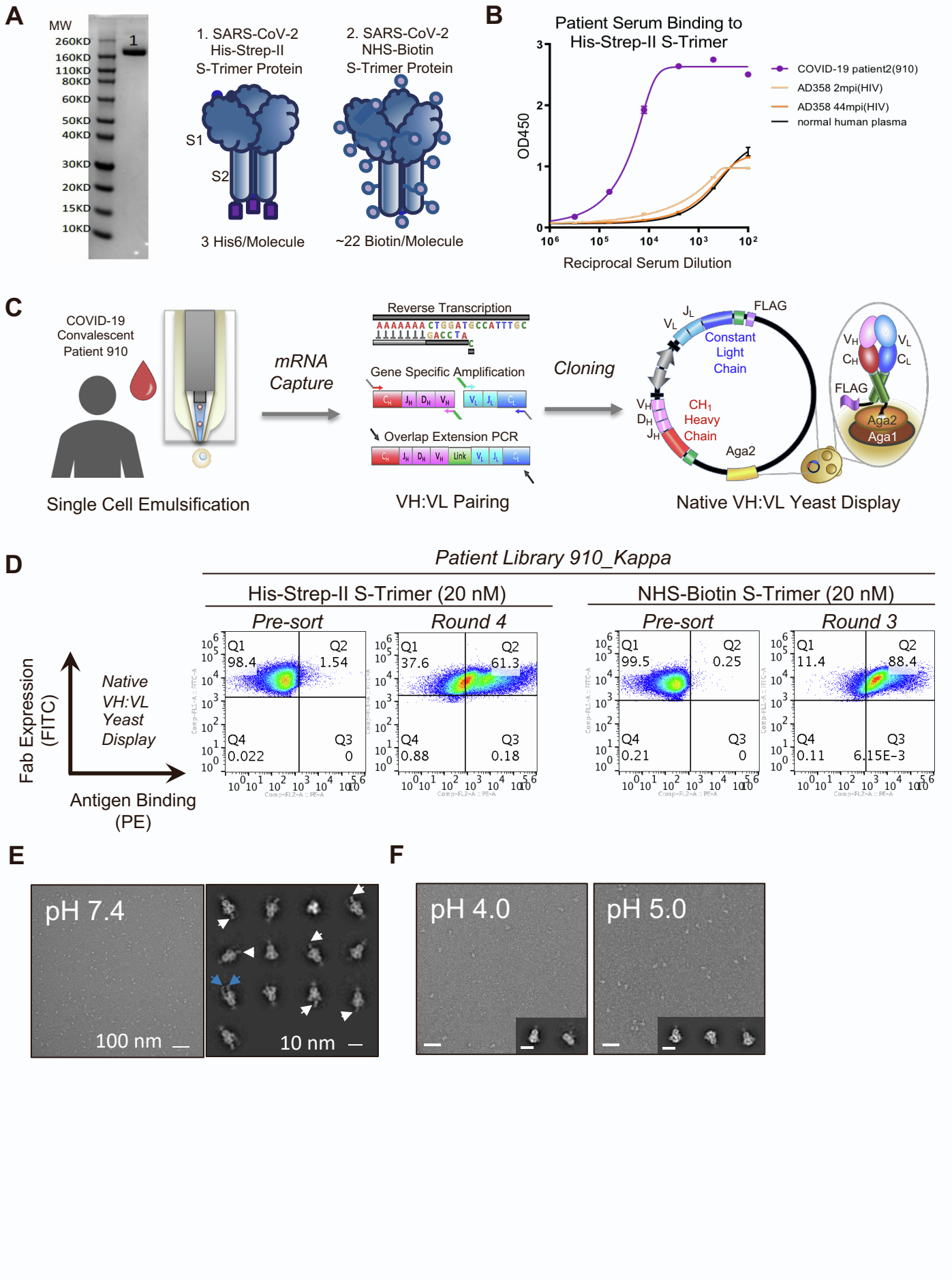
A
MW
260KD
160KD
110KD
80KD
60KD
50KD
40KD
30KD
20KD
15KD
10KD
1
1. SARS-CoV-2
His-Strep-II
S-Trimer Protein
S1
S2
3 His6/Molecule
2. SARS-CoV-2
NHS-Biotin
S-Trimer Protein
~22 Biotin/Molecule
B
Patient Serum Binding to
His-Strep-II S-Trimer
OD450
Reciprocal Serum Dilution
COVID-19 patient2(910)
AD358 2mpi(HIV)
AD358 44mpi(HIV)
normal human plasma
C
COVID-19
Convalescent
Patient 910
Single Cell Emulsification
mRNA
Capture
Reverse Transcription
Gene Specific Amplification
Overlap Extension PCR
VH:VL Pairing
Cloning
FLAG
Constant
Light
Chain
CH1
Heavy
Chain
Aga2
Aga1
Native VH:VL Yeast Display
D
Patient Library 910_Kappa
His-Strep-II S-Trimer (20 nM)
NHS-Biotin S-Trimer (20 nM)
Pre-sort
Round 4
Pre-sort
Round 3
Q1 98.4
Q2 1.54
Q4 0.022
Q3 0
Q1 37.6
Q2 61.3
Q4 0.88
Q3 0.18
Q1 99.5
Q2 0.25
Q4 0.21
Q3 0
Q1 11.4
Q2 88.4
Q4 0.11
Q3 6.15E-3
Fab Expression
(FITC)
Native
VH:VL
Yeast
Display
Antigen Binding
(PE)
E
pH 7.4
100 nm
10 nm
F
pH 4.0
pH 5.0

Supplementary Figure 1. Overview of 910-30 discovery from a convalescent COVID-19 patient utilizing natively paired antibody fragment yeast display, FACS bio-panning, and soluble characterization related to Figure 1 and STAR Methods. **(A)** Reduced SDS-PAGE gel shows SARS-CoV-2 His-Strep-II S-Trimer monomer protein at approximately 142 kDa. Schematics highlight unique features of SARS-CoV-2 Spike S2P antigen probes used for FACS biopanning of antibody yeast display libraries from a COVID-19 convalescent donor. **(B)** Hong Kong University convalescent Donor 910 serum showed strong binding to SARS-CoV-2 His-Strep-II S-Trimer protein compared to controls. Data are represented as mean ± SEM. **(C)** Workflow overview used to generate native VH:VL libraries from the COVID-19 convalescent donor HKU910 for functional antibody screening using yeast display. **(D)** Donor-derived antibody library bio-panning via FACS shows significant library enrichment after multiple rounds of sorting. *Left* Donor 910 pre-sort yeast library vs. sorted yeast library for His-S-Trimer antigen. *Right* Donor 910 pre-sort yeast library vs. sorted yeast library for Biotin-S-Trimer antigen. **(E)** Negative-staining electron microscopy at pH 7.4 resolved complexes between SARS-CoV-2 S2P and 910-30 Fab. Left: representative micrograph; right: representative 2D class averages. White arrows point to Fab fragments in complexes formed between one Fab and one spike trimer; blue arrows point to Fab fragments in complexes formed between two Fab fragments and one spike trimer. **(F)** Negative-staining electron microscopy at pH 4.0, and 5.0 reveal no 910-30 Fab bound to SARS-CoV-2 S2P protein at given pH values. Representative micrographs are shown. Insets show representative 2D class averages. Scale bars: 50 nm (micrographs), 20 nm (2D class averages).

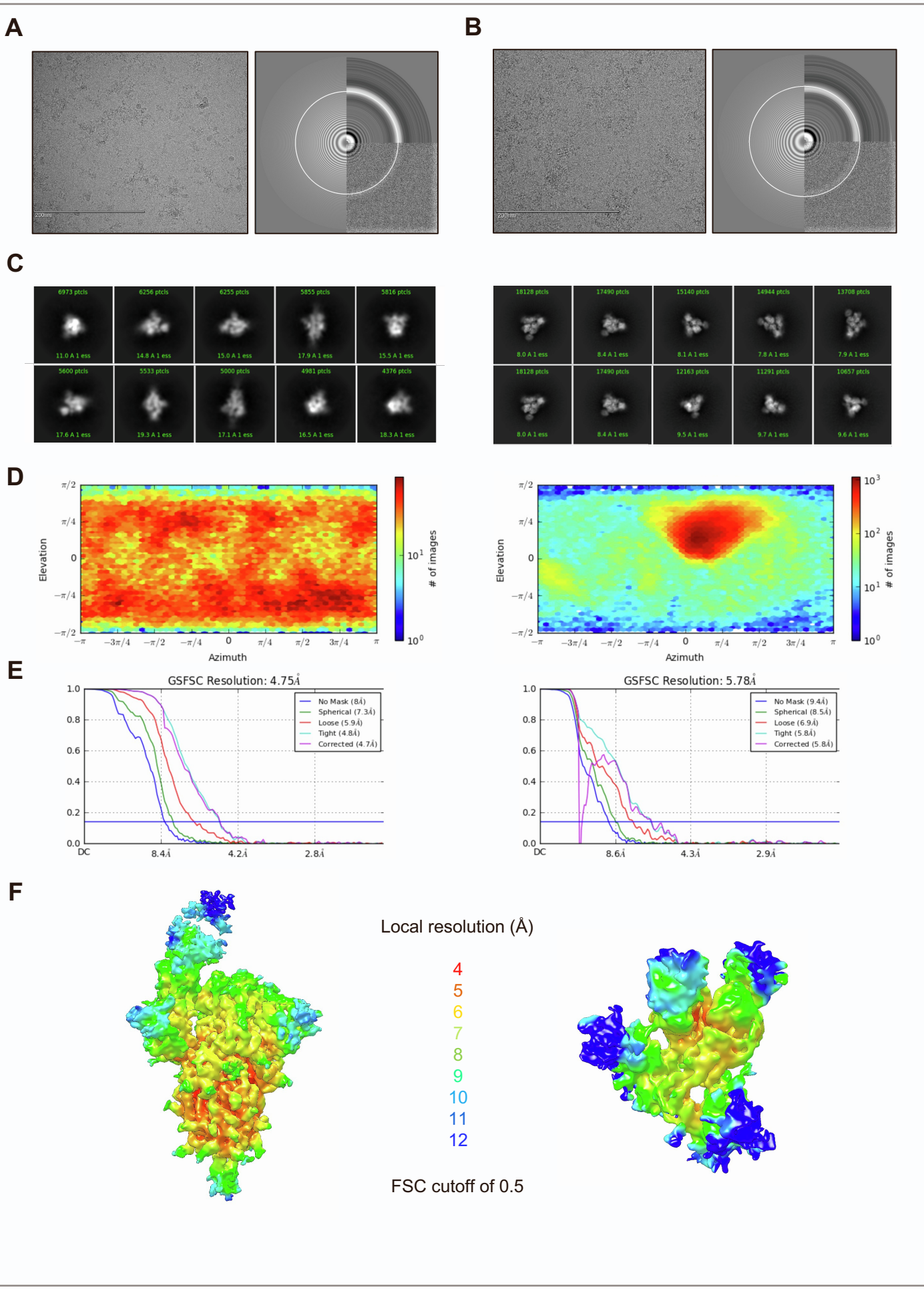
A
B
C
6973 ptcls
6256 ptcls
6255 ptcls
5855 ptcls
5816 ptcls
11.0 A 1 ess
14.8 A 1 ess
15.0 A 1 ess
17.9 A 1 ess
15.5 A 1 ess
5600 ptcls
5533 ptcls
5000 ptcls
4981 ptcls
4376 ptcls
17.6 A 1 ess
19.3 A 1 ess
17.1 A 1 ess
16.5 A 1 ess
18.3 A 1 ess
18128 ptcls
17490 ptcls
15140 ptcls
14944 ptcls
13708 ptcls
8.0 A 1 ess
8.4 A 1 ess
8.1 A 1 ess
7.8 A 1 ess
7.9 A 1 ess
18128 ptcls
17490 ptcls
12163 ptcls
11291 ptcls
10657 ptcls
8.0 A 1 ess
8.4 A 1 ess
9.5 A 1 ess
9.7 A 1 ess
9.6 A 1 ess
D
Elevation
Azimuth
# of images
E
GSFSC Resolution: 4.75Å
No Mask (8Å)
Spherical (7.3Å)
Loose (5.9Å)
Tight (4.8Å)
Corrected (4.7Å)
GSFSC Resolution: 5.78Å
No Mask (9.4Å)
Spherical (8.5Å)
Loose (6.9Å)
Tight (5.8Å)
Corrected (5.8Å)
F
Local resolution (Å)
4
5
6
7
8
9
10
11
12
FSC cutoff of 0.5

Supplementary Figure 2. Cryo-EM analysis of 910-30 Fab in complex with SARS-CoV-2 spike at pH 5.5. Sample 1 obtained mixing 910-30 Fab and spike in a 1:1 molar ratio, sample 2 obtained mixing 910-30 Fab and spike in a 9:1 molar ratio. Related to Figures 1C and 1D. (A) Representative micrograph and CTF of the micrograph for sample 1. **(B)** Representative micrograph and CTF of the micrograph for sample 2. **(C)** Representative 2D classes for sample 1 (left) and sample 2 (right). **(D)** The orientations of all particles used in the final refinement are shown as a heatmap for sample 1 (left) and sample 2 (right). **(E)** The gold-standard Fourier shell correlation resulted in a resolution of 4.75 Å for sample 1 (left) and 5.78 Å for sample 2 (right). **(F)** The local resolution of the two final maps are shown generated through cryoSPARC using an FSC cutoff of 0.5; left: sample 1, right: sample 2.

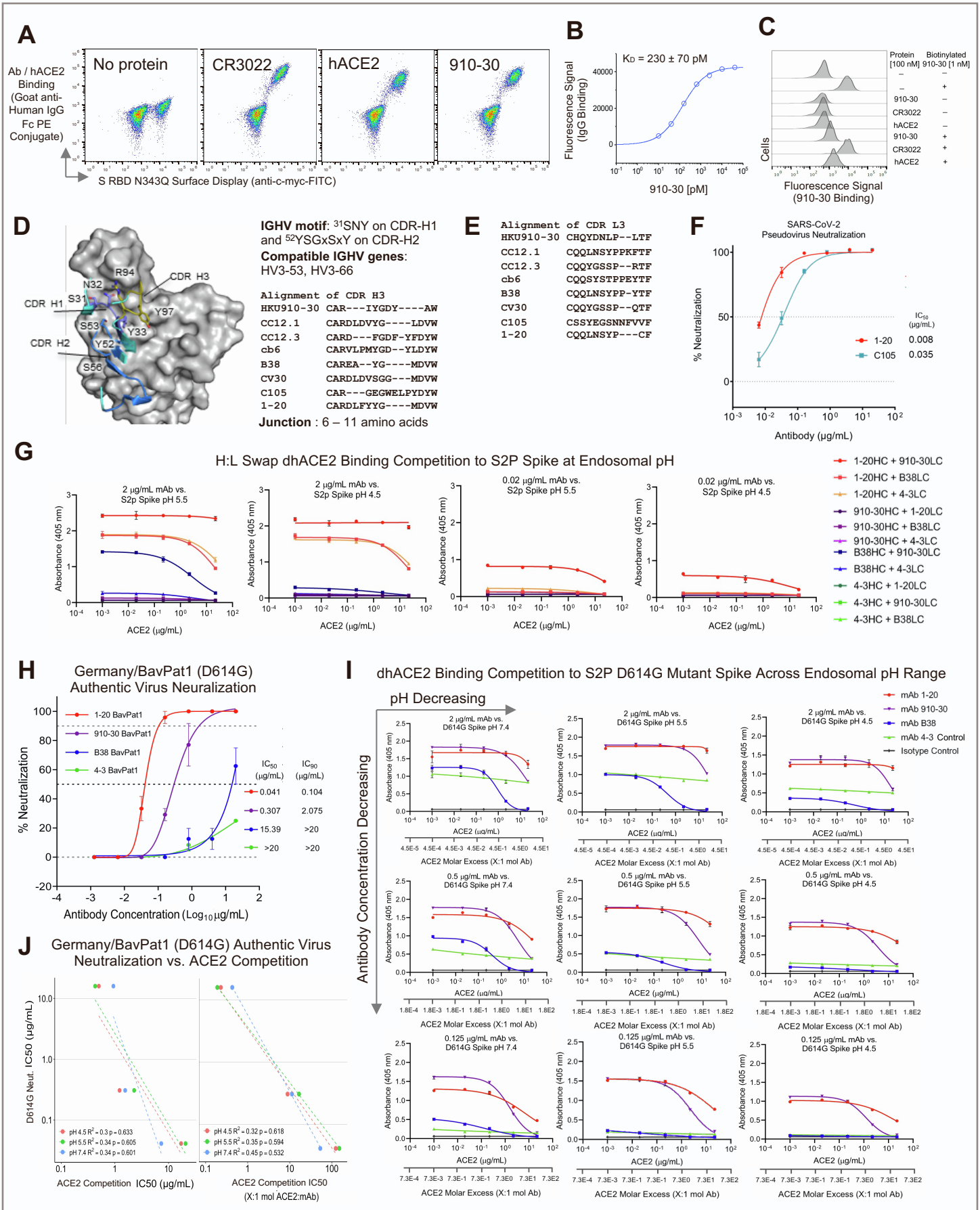
A
Ab / hACE2 Binding (Goat anti-Human IgG Fc PE Conjugate)
No protein
CR3022
hACE2
910-30
S RBD N343Q Surface Display (anti-c-myc-FITC)
B
KD = 230 ± 70 pM
Fluorescence Signal (IgG Binding)
910-30 [pM]
C
Protein [100 nM]
Biotinylated 910-30 [1 nM]
910-30
CR3022
hACE2
Cells
Fluorescence Signal (910-30 Binding)
D
R94
CDR H3
N32
S31
CDR H1
Y97
S53
Y33
CDR H2
Y52
S56
IGHV motif: 31SNY on CDR-H1 and 52YSGxSxY on CDR-H2
Compatible IGHV genes: HV3-53, HV3-66
Alignment of CDR H3
HKU910-30 CAR---IYGDY----AW
CC12.1 CARDLDVYG----LDVW
CC12.3 CARD---FGDF-YFDYW
cb6 CARVLPMYGD--YLDYW
B38 CAREA--YG----MDVW
CV30 CARDLDVSGG---MDVW
C105 CAR---GEGWELPYDYW
1-20 CARDLFYYG----MDVW
Junction : 6 – 11 amino acids
E
Alignment of CDR L3
HKU910-30 CHQYDNLP--LTF
CC12.1 CQQLNSYPPKFTF
CC12.3 CQQYGSSP--RTF
cb6 CQQSYSTPPEYTF
B38 CQQLNSYPP-YTF
CV30 CQQYGSSP--QTF
C105 CSSYEGSNNFVVF
1-20 CQQLNSYP---CF
F
SARS-CoV-2 Pseudovirus Neutralization
% Neutralization
Antibody (μg/mL)
IC50 (μg/mL)
1-20 0.008
C105 0.035
G
H:L Swap dhACE2 Binding Competition to S2P Spike at Endosomal pH
2 μg/mL mAb vs. S2p Spike pH 5.5
2 μg/mL mAb vs. S2p Spike pH 4.5
0.02 μg/mL mAb vs. S2p Spike pH 5.5
0.02 μg/mL mAb vs. S2p Spike pH 4.5
Absorbance (405 nm)
ACE2 (μg/mL)
1-20HC + 910-30LC
1-20HC + B38LC
1-20HC + 4-3LC
910-30HC + 1-20LC
910-30HC + B38LC
910-30HC + 4-3LC
B38HC + 910-30LC
B38HC + 4-3LC
4-3HC + 1-20LC
4-3HC + 910-30LC
4-3HC + B38LC
H
Germany/BavPat1 (D614G) Authentic Virus Neuralization
1-20 BavPat1
910-30 BavPat1
B38 BavPat1
4-3 BavPat1
% Neutralization
IC50 (μg/mL)
IC90 (μg/mL)
0.041 0.104
0.307 2.075
15.39 >20
>20 >20
Antibody Concentration (Log10 μg/mL)
I
dhACE2 Binding Competition to S2P D614G Mutant Spike Across Endosomal pH Range
pH Decreasing
Antibody Concentration Decreasing
2 μg/mL mAb vs. D614G Spike pH 7.4
2 μg/mL mAb vs. D614G Spike pH 5.5
2 μg/mL mAb vs. D614G Spike pH 4.5
0.5 μg/mL mAb vs. D614G Spike pH 7.4
0.5 μg/mL mAb vs. D614G Spike pH 5.5
0.5 μg/mL mAb vs. D614G Spike pH 4.5
0.125 μg/mL mAb vs. D614G Spike pH 7.4
0.125 μg/mL mAb vs. D614G Spike pH 5.5
0.125 μg/mL mAb vs. D614G Spike pH 4.5
Absorbance (405 nm)
ACE2 (μg/mL)
ACE2 Molar Excess (X:1 mol Ab)
mAb 1-20
mAb 910-30
mAb B38
mAb 4-3 Control
Isotype Control
J
Germany/BavPat1 (D614G) Authentic Virus Neutralization vs. ACE2 Competition
D614G Neut. IC50 (μg/mL)
pH 4.5 R2 = 0.3 p = 0.633
pH 5.5 R2 = 0.34 p = 0.605
pH 7.4 R2 = 0.34 p = 0.601
pH 4.5 R2 = 0.32 p = 0.618
pH 5.5 R2 = 0.35 p = 0.594
pH 7.4 R2 = 0.45 p = 0.532
ACE2 Competition IC50 (μg/mL)
ACE2 Competition IC50 (X:1 mol ACE2:mAb)

Supplementary Figure 3. IGHV3-53/3-66 class member extended characterization and biophysical analysis related to Figures 2, 3, and 4. (A) Yeast-displayed aglycosylated RBD demonstrates 910-30 recognition is glycan-independent. S RBD N343Q with a C-terminal myc epitope tag was displayed on the surface of yeast and labeled with no protein or 1 nM of CR3022, human ACE2-Fc (hACE2), or 910-30. Cells were washed, secondarily labeled with anti-c-myc-FITC and Goat anti-Human IgG Fc PE conjugate, and read on a Sony SH800 cell sorter. Biological replicates were performed on two different days. **(B)** Yeast cell surface titrations of 910-30 IgG against aglycosylated S RBD yield a K_D of 230 ± 38 pM. Technical triplicates were performed for two biological replicates (n = 6), and error reported is 2 s.e.m. **(C)** Yeast-displayed RBD competition binding experiments of free 910-30, hACE2 and CR3022 vs. biotinylated or unbiotinylated 910-30. Technical triplicates were performed for two biological replicates (n = 6). **(D)** Heavy chain genetic elements associated with the IGHV3-53/3-66 antibody class. **(E)** Light chain CDR3 alignment of IGHV3-53/3-66 antibody class. **(F)** Lambda chain IGHV3-53/3-66 class member C105 shows moderate neutralizing capacity compared to potent kappa chain IGHV3-53/3-66 class member 1-20. Data are represented as mean ± SEM. **(G)** pH mediated dhACE2 competition measured by ELISA showing constant concentrations of heavy-light-swapped IgG binding to SARS-CoV-2 S2P protein versus increasing dhACE2 (ACE2) concentrations. Potently neutralizing heavy-light swap variants (Fig. 3A) show higher affinity binding to S2P spike and stronger ACE2 competition relative to less potent Abs. Data are represented as mean ± SEM. **(H)** 1-20, 910-30, and B38 show equivalent neutralization in a D614G authentic virus assay as for D614 authentic virus (Fig. 2D), with 4-3 included as a gene-matched control. Data are represented as mean ± SEM. **(I)** SARS-CoV-2 D614G S2P protein mutant variant pH mediated dhACE2 (ACE2) competition measured by ELISA showing constant concentrations of heavy-light-swapped IgG versus increasing dhACE2 concentrations. Potently neutralizing heavy-light swap variants show higher affinity binding to D614G S2P mutant spike and stronger ACE2 competition relative to less potent Abs. The concentration of dhACE2 required to outcompete antibody binding to spike is given as both μg/mL and as ACE2 molar excess units. Data are represented as mean ± SEM. **(J)** D614G authentic virus neutralization potency (Fig. S4H) and dhACE2 competition IC_{50} (Fig. S4I) show a correlation between potent neutralization and stronger ACE2 competition.

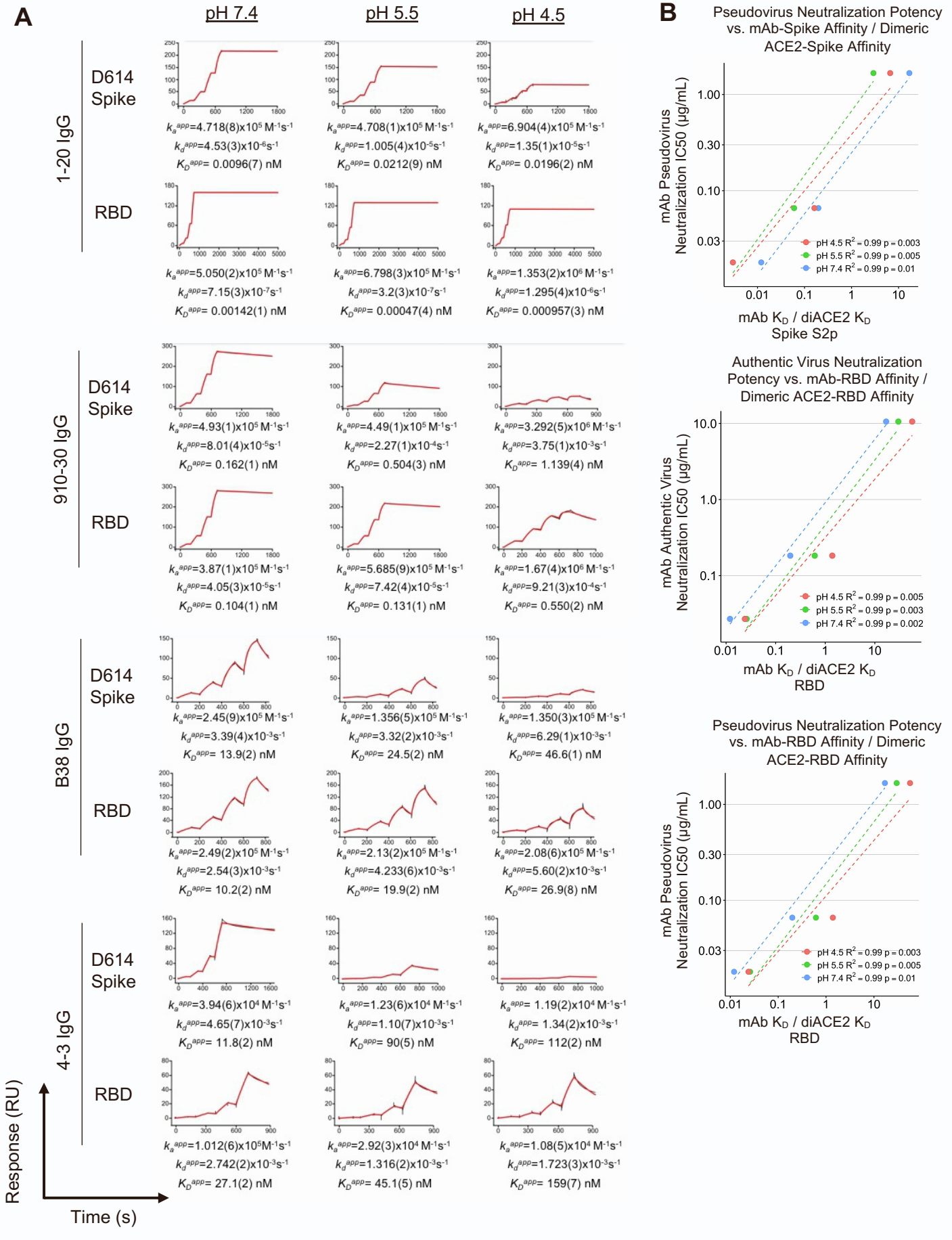
A
pH 7.4
pH 5.5
pH 4.5
1-20 IgG
D614 Spike
k_a^{app}=4.718(8)x10^5 M^{-1}s^{-1}
k_d^{app}=4.53(3)x10^{-6}s^{-1}
K_D^{app}= 0.0096(7) nM
k_a^{app}=4.708(1)x10^5 M^{-1}s^{-1}
k_d^{app}=1.005(4)x10^{-5}s^{-1}
K_D^{app}= 0.0212(9) nM
k_a^{app}=6.904(4)x10^5 M^{-1}s^{-1}
k_d^{app}=1.35(1)x10^{-5}s^{-1}
K_D^{app}= 0.0196(2) nM
RBD
k_a^{app}=5.050(2)x10^5 M^{-1}s^{-1}
k_d^{app}=7.15(3)x10^{-7}s^{-1}
K_D^{app}= 0.00142(1) nM
k_a^{app}=6.798(3)x10^5 M^{-1}s^{-1}
k_d^{app}=3.2(3)x10^{-7}s^{-1}
K_D^{app}= 0.00047(4) nM
k_a^{app}=1.353(2)x10^6 M^{-1}s^{-1}
k_d^{app}=1.295(4)x10^{-6}s^{-1}
K_D^{app}= 0.000957(3) nM
910-30 IgG
D614 Spike
k_a^{app}=4.93(1)x10^5 M^{-1}s^{-1}
k_d^{app}=8.01(4)x10^{-5}s^{-1}
K_D^{app}= 0.162(1) nM
k_a^{app}=4.49(1)x10^5 M^{-1}s^{-1}
k_d^{app}=2.27(1)x10^{-4}s^{-1}
K_D^{app}= 0.504(3) nM
k_a^{app}=3.292(5)x10^6 M^{-1}s^{-1}
k_d^{app}=3.75(1)x10^{-3}s^{-1}
K_D^{app}= 1.139(4) nM
RBD
k_a^{app}=3.87(1)x10^5 M^{-1}s^{-1}
k_d^{app}=4.05(3)x10^{-5}s^{-1}
K_D^{app}= 0.104(1) nM
k_a^{app}=5.685(9)x10^5 M^{-1}s^{-1}
k_d^{app}=7.42(4)x10^{-5}s^{-1}
K_D^{app}= 0.131(1) nM
k_a^{app}=1.67(4)x10^6 M^{-1}s^{-1}
k_d^{app}=9.21(3)x10^{-4}s^{-1}
K_D^{app}= 0.550(2) nM
B38 IgG
D614 Spike
k_a^{app}=2.45(9)x10^5 M^{-1}s^{-1}
k_d^{app}=3.39(4)x10^{-3}s^{-1}
K_D^{app}= 13.9(2) nM
k_a^{app}=1.356(5)x10^5 M^{-1}s^{-1}
k_d^{app}=3.32(2)x10^{-3}s^{-1}
K_D^{app}= 24.5(2) nM
k_a^{app}=1.350(3)x10^5 M^{-1}s^{-1}
k_d^{app}=6.29(1)x10^{-3}s^{-1}
K_D^{app}= 46.6(1) nM
RBD
k_a^{app}=2.49(2)x10^5 M^{-1}s^{-1}
k_d^{app}=2.54(3)x10^{-3}s^{-1}
K_D^{app}= 10.2(2) nM
k_a^{app}=2.13(2)x10^5 M^{-1}s^{-1}
k_d^{app}=4.233(6)x10^{-3}s^{-1}
K_D^{app}= 19.9(2) nM
k_a^{app}=2.08(6)x10^5 M^{-1}s^{-1}
k_d^{app}=5.60(2)x10^{-3}s^{-1}
K_D^{app}= 26.9(8) nM
4-3 IgG
D614 Spike
k_a^{app}=3.94(6)x10^4 M^{-1}s^{-1}
k_d^{app}=4.65(7)x10^{-3}s^{-1}
K_D^{app}= 11.8(2) nM
k_a^{app}=1.23(6)x10^4 M^{-1}s^{-1}
k_d^{app}=1.10(7)x10^{-3}s^{-1}
K_D^{app}= 90(5) nM
k_a^{app}= 1.19(2)x10^4 M^{-1}s^{-1}
k_d^{app}= 1.34(2)x10^{-3}s^{-1}
K_D^{app}= 112(2) nM
RBD
k_a^{app}=1.012(6)x10^{5}M^{-1}s^{-1}
k_d^{app}=2.742(2)x10^{-3}s^{-1}
K_D^{app}= 27.1(2) nM
k_a^{app}=2.92(3)x10^4 M^{-1}s^{-1}
k_d^{app}=1.316(2)x10^{-3}s^{-1}
K_D^{app}= 45.1(5) nM
k_a^{app}=1.08(5)x10^4 M^{-1}s^{-1}
k_d^{app}=1.723(3)x10^{-3}s^{-1}
K_D^{app}= 159(7) nM
Response (RU)
Time (s)
B
Pseudovirus Neutralization Potency vs. mAb-Spike Affinity / Dimeric ACE2-Spike Affinity
mAb Pseudovirus Neutralization IC50 (µg/mL)
1.00
0.30
0.10
0.03
pH 4.5 R^2 = 0.99 p = 0.003
pH 5.5 R^2 = 0.99 p = 0.005
pH 7.4 R^2 = 0.99 p = 0.01
0.01
0.1
1
10
mAb K_D / diACE2 K_D
Spike S2p
Authentic Virus Neutralization Potency vs. mAb-RBD Affinity / Dimeric ACE2-RBD Affinity
mAb Authentic Virus Neutralization IC50 (µg/mL)
10.0
1.0
0.1
pH 4.5 R^2 = 0.99 p = 0.005
pH 5.5 R^2 = 0.99 p = 0.003
pH 7.4 R^2 = 0.99 p = 0.002
0.01
0.1
1
10
mAb K_D / diACE2 K_D
RBD
Pseudovirus Neutralization Potency vs. mAb-RBD Affinity / Dimeric ACE2-RBD Affinity
mAb Pseudovirus Neutralization IC50 (µg/mL)
1.00
0.30
0.10
0.03
pH 4.5 R^2 = 0.99 p = 0.003
pH 5.5 R^2 = 0.99 p = 0.005
pH 7.4 R^2 = 0.99 p = 0.01
0.01
0.1
1
10
mAb K_D / diACE2 K_D
RBD

Supplementary Figure 4. Extended binding and neutralization analysis across multiple pH values related to Figures 4C and 4D. (A) pH mediated SPR single-cycle kinetic experiments for 910-30, B38, 4-3, and 1-20, for IgG binding to biotinylated spike (top row) and to biotinylated-RBD (bottom row) in each of the four panels. Black traces represent the experimental data and red traces represent the fit to a 1:1 interaction model. The number in brackets represents the error of the fit in the last significant digit. **(B)** Correlations between both authentic and pseudovirus neutralization vs. the ratio of antibody IgG affinity to RBD or Spike divided by dimeric ACE2 affinity to RBD or Spike.

Supplementary Table 1. Cryo-EM data collection and refinement statistics for 910-30 Fab in complex with SARS-CoV-2 spike at pH 5.5 related to Figure 1D.

	SARS-CoV-2 spike in complex with 910-30 Fab at pH 5.5 (folded spike)	SARS-CoV-2 spike in complex with 910-30 Fab at pH 5.5 (disrupted spike)
EMDB ID	EMD-23016	EMD-23039
PDB ID	7KS9	
Data Collection		
Microscope	FEI Titan Krios	FEI Titan Krios
Voltage (kV)	300	300
Electron dose ($e^-/Å^2$)	41.92	41.92
Detector	Gatan K3 BioQuantum	Gatan K3 BioQuantum
Pixel Size (Å)	1.07	1.07
Defocus Range (μm)	-0.8/-2.5	-0.8/-2.5
Magnification	81000	81000
Reconstruction		
Software	cryoSPARC v2.15	cryoSPARC v2.15
Particles	88,315	188,269
Symmetry	C1	C1
Box size (pix)	400	400
Resolution (Å) ($FSC_{0.143}$)	4.75	5.78
Refinement		
Software	Phenix 1.18	
Protein residues	3189	
Chimera CC	0.88	
EMRinger Score	0.55	
R.m.s. deviations		
Bond lengths (Å)	0.003	
Bond angles (°)	0.711	
Validation		
Molprobity score	1.15	
Clash score	3.59	
Favored rotamers (%)	100	
Ramachandran		
Favored regions (%)	98.0	
Allowed regions (%)	2.0	
Disallowed regions (%)	0	

Supplementary Table 2. List of IGHV3-53 / IGHV3-66 anti-SARS-CoV-2 antibodies in previously published articles related to Figure 2B. Supplemental Table provided separately as an Excel file.

Supplementary Table 3. Features of the IGHV3-53/3-66 antibodies investigated in this study related to Figures 2, 3, and 4.

		Antibody			
Feature	Units	1-20	910-30	B38	4-3
Relevant Spike S2P Affinity Values (pH 7.4)	*ka* (M^-1 s^-1)	4.718×10^{5}	4.39×10^{5}	2.45×10^{5}	3.94×10^{4}
	kd (s^-1)	4.53×10^{-6}	8.01×10^{-5}	3.39×10^{-3}	4.65×10^{-3}
	KD (nM)	0.0096	0.162	13.9	11.8
Relevant RBD Affinity Values (pH 7.4)	*ka* (M^-1 s^-1)	5.050×10^{5}	3.87×10^{5}	2.49×10^{5}	1.012×10^{5}
	kd (s^-1)	7.15×10^{-7}	4.05×10^{-5}	2.54×10^{-3}	2.742×10^{-3}
	KD (nM)	0.00142	0.104	10.2	27.1
WT (D614) Pseudo Virus Neutralization potency (µg/mL)	IC50	0.018	0.066	1.668	5.582
WT (D614) Authentic Virus Neutralization potency (µg/mL)	IC50	0.027	0.183	10.571	18.54
	IC90	0.219	1.436	>20	>20
Mutant D614G Authentic Virus Neutralization potency (µg/mL)	IC50	0.041	0.307	15.39	>20
	IC90	0.104	2.075	>20	>20
Heavy chain	IGHV Gene	IGHV3-53*01	IGHV3-53*04	IGHV3-53*04	IGHV3-66*01
	IGHJ Gene	IGHJ6*02	IGHJ5*02	IGHJ6*02	IGHJ6*01 F
	IGHD Gene	IGHD2-2*02	IGHD4-17*01	N/A	IGHD1-26*01
	IGHV identity aa	97.9%	99.0%	99.0%	99.0%
	CDR-H3 seq (aa)	CARDLFYYGMDVW	CARIYGDYAW	CAREAYGMDVW	CARDSSEGPGYYGMDVW
	CDR-H3 len (aa)	13	10	11	17
Light chain	IGKV Gene	IGKV1-9*01	IGKV1-33*01	IGKV1-9*01	IGKV1-9*01
	IGKJ Gene	IGKJ3*01	IGKJ4*01	IGKJ2*01	IGKJ4*01
	IGKV identity aa	100.0%	97.9%	97.9%	100.0%
	CDR-L3 seq (aa)	CQQLNSYPCF	CHQYDNLPLTF	CQQLNSYPPYTF	CQQLNSYLPLTF
	CDR-L3 len (aa)	10	11	12	12

Supplementary Table 4. Heavy chain and light chain CDR1 and CDR2 sequence alignment for recognition signature related to Figures 3C, S3D, and S3E. Supplemental Table provided separately as an Excel file.